VOLITIONAL ACTION, W.A. Hershberger (Editor)

CHAPTER 11
VITE AND FLETE: NEURAL MODULES FOR TRAJECTORY FORMATION AND POSTURAL CONTROL

Daniel Bullock[1] and Stephen Grossberg[2]

1. Factorization Of Pattern And Energy In Trajectory Formation And Tension Control

The modern study of neural networks has shown that even the simplest actions may involve the coordinated activity of millions of biological elements. For example, a simple skeletal action such as rotation around a single joint involves coordinated activity of two muscles, one of which shortens while the other lengthens. Each muscle in turn is composed of a population of contractile fibers and sensory organs, which, respectively, are linked by efferent and afferent nerves with neuronal populations in the spinal cord. These spinal neuron populations are in turn linked, by a bewildering array of descending and ascending pathways, with a large number of discrete supraspinal centers.

Volitional activity may at first seem to belie this complexity, for when we exercise voluntary control, it seems that we do something quite simple. How can voluntary activity appear so simple if every action is inherently so complex? The answer lies in noticing the nature of the control we voluntarily exercise, and also the large range of action parameters over which we lack direct control. We do seem to exercise fairly direct control over where and how fast we move (Sections 2-6), over how forcefully we try to hold a posture (Sections 7-15), even over the vigilance with which we perform tasks (Carpenter & Grossberg, 1987,

---

[1] Supported in part by the National Science Foundation (NSF IRI-87-16960).

[2] Supported in part by the National Science Foundation (NSF IRI-87-16960) and the Air Force Office of Scientific Research (AFOSR F49620-86-C-0037 & AFOSR F49620-87-C-0018).

1988). On the other hand, we do not have direct control over many of the processes that automatically compensate for changes in limb position and inertia during rapid trajectory formation, or that adapt to changes in the parameters of the muscle plant due to exercise, aging, or accidents.

One of the devices whereby voluntary control is simplified is the use of *non-specific* control signals. A nonspecific signal is a scalar signal that is generated at a single command source and broadcast, through a parallel fan-out of pathways, to many target cells. It is then up to the target cells to react appropriately to the widely broadcast signal. If each cell reacts in a state-dependent manner, a nonspecific signal can control an entire array of events without requiring conscious knowledge of the controlled array.

In order for such a simplification of control to work, the target cell array must be appropriately designed. For example, in a real neural network, all neurons have finite activities, or potentials. Broadcasting the same signal to an entire array of cells could raise the baseline level of activity across the array and push the activities of many cells to their maximal potentials. The nonspecific signal could hereby homogenize, or compress, the spatial pattern of cell activities. Because information in a neural network is carried by such spatial patterns, a nonspecific signal could easily become information-destroying.

Thus, any widely broadcast volitional signal could destroy information in the target network unless the target network is designed to automatically compensate for the potentially saturating effects of the nonspecific signal. The target network must guarantee that the volitional signal has its intended modulatory effect without destroying its pattern registration and processing characteristics.

The above mentioned issue has been called the *pattern-energy factorization* problem (Grossberg, 1970, 1973, 1978, 1982) to emphasize that many networks are designed to factor pattern differences from overall activity levels. This problem arises in perceptual and cognitive contexts, no less than during voluntary motor control. In this paper, we will illustrate how pattern-energy factorization is realized within two model networks that may play a role in solving two fundamental problems of motor control: How movements are performed at different intended speeds, and how postures are held at different intended levels of rigidity.

The first network, called the Vector Integration To Endpoint, or VITE model (Bullock & Grossberg, 1986, 1988a), indicates how a scalar signal, called the GO signal, affords voluntary control of movement rate without disrupting the spatial pattern characteristics, such as distance and

direction, of the movement trajectory. We will survey operating characteristics of the VITE network, and describe some of the physiological data that support these properties, notably properties of the GO signal.

The second network model, introduced in Bullock and Grossberg (1988d), is called the FLETE model, as a mnemonic for Factorization of LEngth and TEnsion. It models a part of the spino-muscular system that cooperates with the VITE network to generate the forces needed to ensure that the limb follows the trajectory commanded by the VITE circuit. The general outlines of the trajectory-matching capabilities of the spino-muscular system have been discussed elsewhere (e.g., Gielen & Houk, 1987). We focus here on how to design the circuit to enable holding of an arbitrary posture at multiple levels of rigidity via a scalar signal sent in parallel to the motor channels responsible for posture maintenance. As with the VITE network, the FLETE network indicates how a scalar signal resulting from a voluntary choice can have a desired effect on a high-dimensional target system without knowledge of the characteristics of the target system.

Besides discussing the FLETE network's ability to factorize length from tension despite the tendency of a muscle's tension to covary with its length, we will present physiological evidence for the network's components in the spino-muscular system. The FLETE model's mathematical treatment of the spino-muscular system sheds new light on why certain properties, such as the size principle of motoneuron recruitment (Henneman, 1957, 1985), are so prevalent among vertebrates.

The FLETE model also suggests a new functional interpretation for the Renshaw-mediated recurrent inhibition seen in higher vertebrates. Our analysis of the size principle indicates that recurrent inhibition via the Renshaw-Ia pathway serves a more fundamental function than "controlling the gain of the stretch reflex," the most common textbook statement of its primary role. In particular, we argue that this pathway compensates for a threat to postural stability that occurs when the size principle is combined with the co-contractive signals needed to control postural rigidity.

Rather than contradicting other views, our new account helps complete the picture of Renshaw function, and broadens the theoretical context for understanding how "supra-spinal convergence on Renshaw cells allows recurrent inhibition to serve as a variable gain regulator" (Hultborn, Lindstrom, & Wigstrom, 1979) for the final common path. In particular, we make novel predictions regarding supraspinal Renshaw

modulation during postural versus movement states by showing through computer simulations that the desirable decoupling of alpha-motoneuron and Renshaw activities observed in some movement contexts (Pierrot-Deseilligny & Morin, 1980) would be disastrous in many postural contexts.

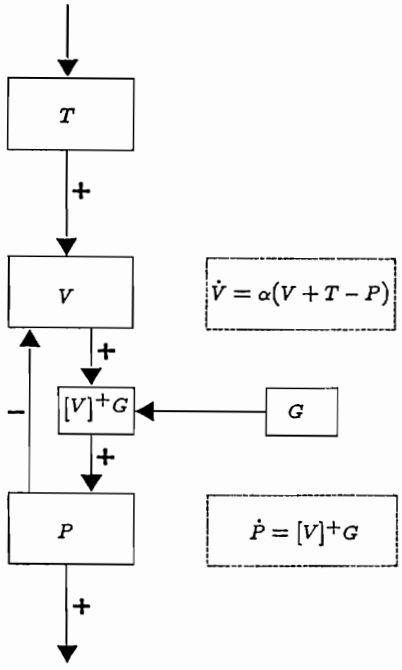

Figure 1. Main variables of the VITE circuit: T = target position command, V = difference vector, G = GO signal, P = present position command. The circuit does not include the opponent interactions that exist between the VG and P stages of agonist and antagonist muscle commands. For these interactions, see Figure 2.

2. Emergent Invariants Of The Vite Circuit

In the VITE model, motor planning occurs in the form of a Target Position Command, or TPC, an array that specifies the lengths to which all trajectory-controlling muscles are intended to move, and an independently controlled GO command, which specifies the movement's overall speed. Automatic processes convert this information into an arm trajectory with invariant properties, notably properties of synchrony among muscle synergists. These automatic processes include computation of a Present Position Command, or PPC, and a Difference Vector, or DV. The DV is the difference between the TPC array and the PPC array at any time. The PPC is gradually updated by integrating the DV through time. A time-varying GO signal multiplies, or gates, the DV before it is integrated by the PPC. The PPC generates an outflow movement

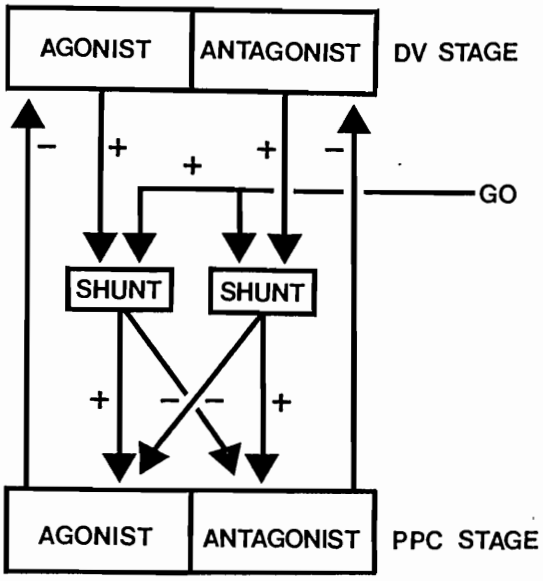

Figure 2. Opponent interactions among VITE circuit channels controlling agonists and their antagonists enable coordinated, automatic updating of their present-position commands (PPCs). Outputs from the PPC stage serve as the basis for reciprocal control of opponent muscles' contractile states.

command to motoneurons controlling its target muscle groups and sends a corollary discharge (inhibitory efference copy) back to the DV stage (Figure 1). Opponent interactions are also needed to regulate the PPC's to agonist and antagonist muscle groups at each joint (Figure 2).

To generate a movement, a TPC different from the current PPC is instated. This generates a non-zero DV which is multiplied by the GO signal to generate an input to the PPC. The PPC integrates this signal through time until the PPC equals the TPC. The model hereby explicates how a limb is commanded to reach the same goal (TPC) from arbitrary initial states (initial PPCs) at variable rates (determined by the size of the GO signal).

In its simplest form, excluding terms expressing opponent interactions, the VITE circuit obeys the equations:

Difference Vector

$$\frac{d}{dt} V_i = \alpha(-V_i + T_i - P_i) \tag{1}$$

and

Present Position Command

$$\frac{d}{dt} P_i = G[V_i]^+, \tag{2}$$

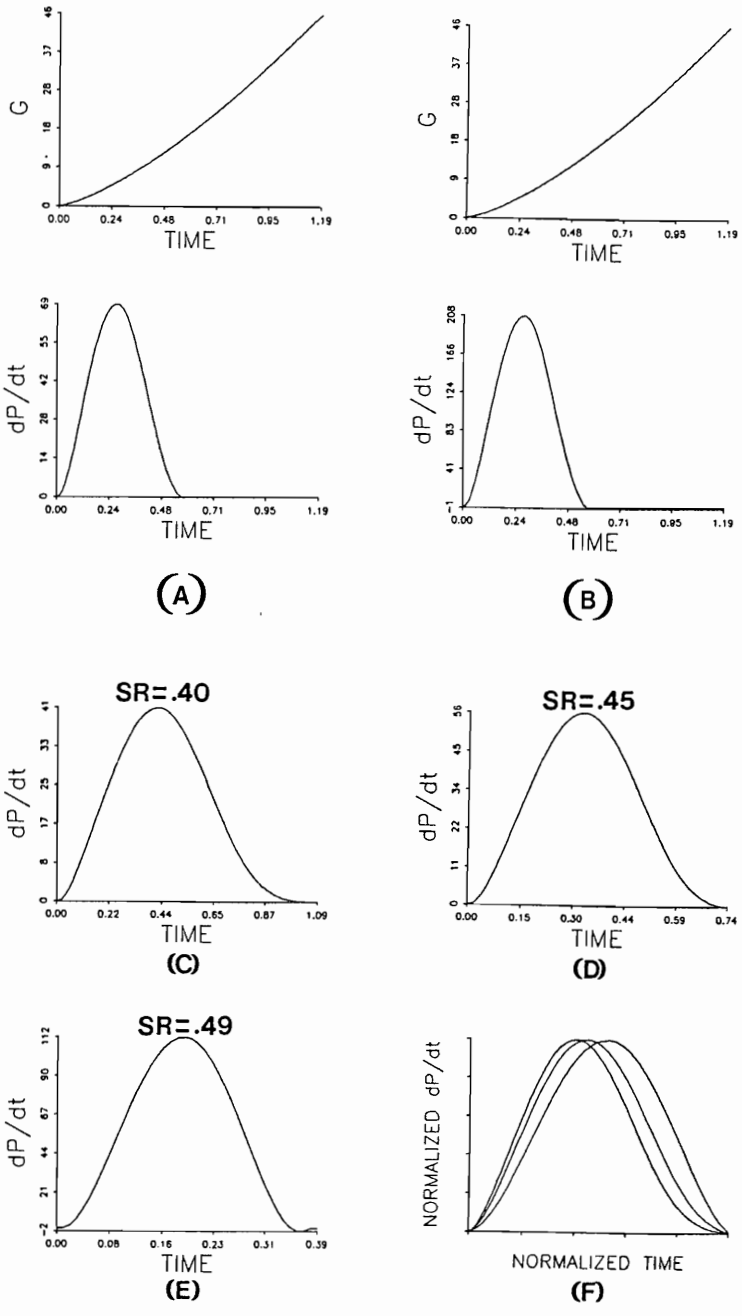

Figure 3. (A,B): With equal GO signals, movements of different size have equal durations and perfectly superimposable velocity profiles after velocity axis rescaling. Shown are GO signals and velocity profiles for 20 and 60 unit movements lasting 500 ms. (C,D,E): Velocity profiles associated with small, medium, and large GO magnitudes result in slow, medium, and fast performance of a 20 unit movement. Each SR value gives the trajectory's *symmetry ratio*; that is, the time taken to move half the distance divided by the total movement duration. These ratios indicate progressive symmetrization at higher speeds, within the range of speeds shown. (F): The velocity profiles shown in (C), (D), and (E) are not perfectly superimposable after time and velocity normalization.

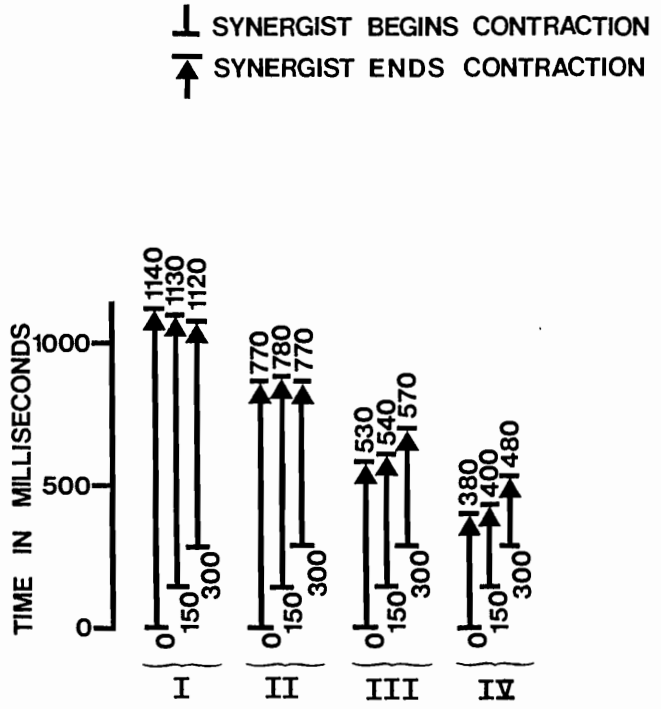

Figure 4. Simulation results showing contraction offset times for three synergistic muscles with different onset times, as a function of the GO signal scalar (the voluntarily chosen multiplier of the time-varying GO signal). In each block, the DV component corresponding to muscle one begins to be read out 0 ms after the start of GO signal buildup, muscle two 150 ms after the start of GO buildup, and muscle three 300 ms after the start of GO buildup. The GO signal scalar was 10, 20, 40, and 80 in blocks I-IV, respectively. Results indicate automatic VITE circuit compensation for staggering of contraction onset times.

where α is a positive constant and $[V_i]^+ = \max(V_i, 0)$. Equations (1) and (2) describe interactions of a generic component of a target position command $(T_1, T_2, \ldots, T_n)$, a difference vector $(V_1, V_2, \ldots, V_n)$, a present position command $(P_1, P_2, \ldots, P_n)$, and a time-varying velocity command, or GO signal $G(t) \geq 0$. The difference vector computes a mismatch between target position and present position, and is used to update present position at a variable rate determined by $G(t)$ until the present position matches the target position. The GO signal is thus a nonspecific command, and the circuit as a whole factors *pattern*, in the form of a vector $(T_1, T_2, \ldots, T_n)$, and *energy*, in the form of a scalar $G(t)$. Because the updating rate for each PPC component P_i is a function of the corresponding DV component V_i, such a scheme permits multiple muscles to contract synchronously even though the total amount of contraction, scaled by $T_i(0) - P_i(0)$, may be different for each effector (Figure 3).

Because the GO signal multiplies the DV signal (Equation 2) on its way to the PPC stage, the VITE circuit is capable of *motor priming.* In particular, even if a new TPC is instated causing a new DV to be computed, there will be no PPC updating until $G(t)$ becomes greater than zero. A new target may hereby be primed before it is released by a volitional act that generates a positive GO signal. Variable speed control and motor priming are thus intimately linked in the VITE model.

In addition, the interaction between the DV and GO signal provides automatic compensation for staggered onset times of synergetic muscles. As shown in Figure 4, even if motor commands to different muscles in a

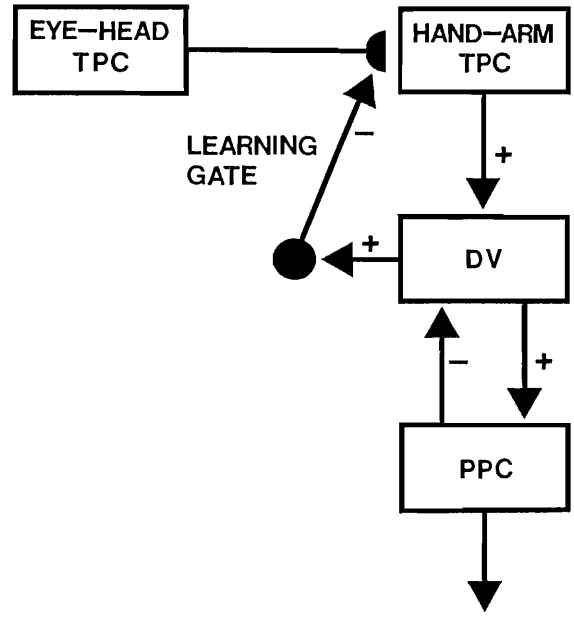

Figure 5. Learning of an intermodal associative transformation between target position maps is gated by a DV process which matches TPC with PPC to prevent incorrect associations from forming between eye-head TPC's and hand-arm TPC's. Learning only occurs when the DV is small.

synergy are initiated at very different times, the times at which all the PPCs reach their target TPCs are much more synchronous. This property may help to generate linear hand-movement paths (Hollerbach, Moore, & Atkeson, 1986). It is also needed to execute motor plans involving a rapid series of movements, because asynchrony in the completion of one movement in the series could destabilize the correct execution of the next movement in the series.

The VITE circuit generates trajectories without regard to the forces required to realize those trajectories. It is not sufficient in itself to accomplish all the tasks required of a variable-speed, variable-load limb movement system. In particular, a key difference between the VITE model and many other model proposals is that the PPC movement command is based on outflow, or feedforward, signals, not inflow, or feedback, signals from the muscles. The process of guaranteeing that the PPC command actually moves the limb to a corresponding position in space is accomplished, in part, by a separate muscle linearization network (MLN) that does use inflow signals in the form of outflow-inflow mismatches to generate error signals that adaptively alter the gain of the total outflow movement command (Grossberg & Kuperstein, 1986, 1989). The cerebellum has been implicated as the locus of adaptive gain change in this model. For arm movements, the VITE circuit and an MLN circuit operate in parallel with the spino-muscular FLETE model system to realize flexible and adaptive trajectories free from the rigid performance inherent in systems that preplan an entire trajectory before beginning to generate the forces needed to implement it.

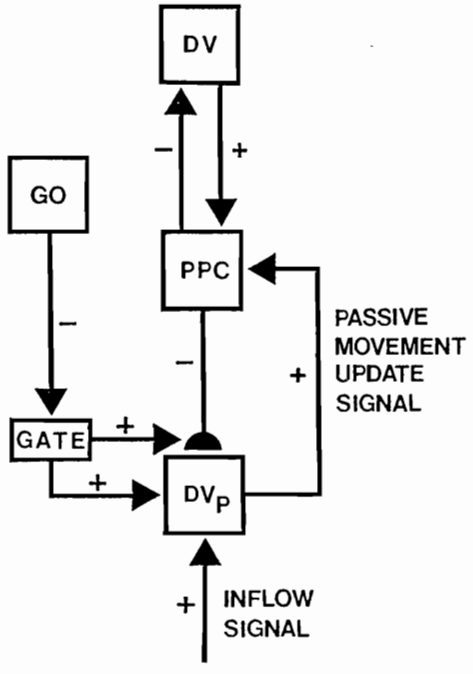

Figure 6. A passive update of position (PUP) circuit. An adaptive pathway $PPC \rightarrow DV_p$ calibrates PPC-outflow signals in the same scale as inflow signals during intervals of posture. During passive movements, output from GO equals zero. Hence the passive difference vector DV_p updates the PPC until it equals the new position caused by any passive movements that may occur due to the application of external forces.

3. Actively Gated Learning Of Target Position And Present Position

In addition to their role in trajectory formation, TPC, PPC, and DV computations are predicted to actively modulate, or gate, the learning of associative maps between TPC's of different modalities, such as between the eye-head system and the hand-arm system (Figure 5) in a manner consistent with Piaget's (1963) analysis of how circular reactions promote map learning. The gating process prevents learning from occurring except when the PPC is close to the TPC; that is, except when the DV is small. Such gating helps to prevent spurious correlations from being learned, say between a fixed target position of the hand and all present positions which the eye assumes while moving to look at the hand. By using such an intermodality associative map, looking at an object can activate a TPC of the eye-head system that is associatively mapped into an appropriate TPC of the hand-arm system, as in the recent model of Kuperstein (1988). A VITE circuit translates this latter TPC into a synchronous movement command for moving the hand to the object.

Active gating is also needed to regulate updating and learning of present position commands during passive arm movements. In particular, an auxiliary circuit, called the Passive Update of Position, or PUP, Model uses inflow signals to update the PPC during passive arm movements due to external forces (Figure 6), but not during active arm movements or during actively maintained posture. Because the scales of outflow position command signals P_i and inflow position sensing signals I_i cannot be assumed to be the same, the PUP circuit incorporates a synaptic modification mechanism for adaptively recalibrating the gain z_i of the PPC outflow signals that are matched with inflow signals until they are computed in the same numerical scale, thereby ensuring that the PUP circuit accurately updates the PPC.

When the VITE Model and PUP Model are combined, the following equations result:

Difference Vector

$$\frac{d}{dt} V_i = \alpha(-V_i + T_i - P_i) \tag{1}$$

Present Position Command

$$\frac{d}{dt} P_i = G[V_i]^+ + G_p[M_i]^+ \tag{3}$$

Outflow-Inflow Match

$$\frac{d}{dt} M_i = -\beta M_i + \gamma I_i - z_i P_i \tag{4}$$

Adaptive Gain Control

$$\frac{d}{dt} z_i = \delta G_p(-\epsilon z_i + [M_i]^+). \tag{5}$$

Active and Passive GO Signals

$$G + G_p > 0 \text{ and } GG_p = 0 \tag{6}$$

Equation (3) supplements equation (2) with a position update signal $G_p[M_i]^+$. This signal is turned on only when the passive GO signal gating function, or "pauser" signal, G_p becomes positive as G becomes zero in (6), and when the outflow-inflow match function $M_i>0$. Equation (4) shows that $M_i>0$ only when the outflow signal, $z_i P_i$, is less than the inflow signal, γI_i . Function z_i in (5) is a long term memory trace, or associative weight, which adaptively recalibrates the gain of outflow signals P_i until they are in the same scale as inflow signals γI_i in (4). Then the match function M_i is able to update the PPC in equation (3) until it accurately registers the new position caused by external forces.

In summary, offset of the GO signal within the VITE circuit enables a pauser signal within the PUP circuit to drive its learning and reset functions. Such pauser-modulated learning during mismatches has been suggested to occur in several adaptive sensory-motor control circuits (Bullock & Grossberg, 1988c; Grossberg and Kuperstein, 1986, 1989). Onset of the GO signal is also suggested to inhibit inflow channels controlling "long-loop" postural reflexes, which would disrupt trajectory formation if allowed to function during fast movements (Evarts & Fromm, 1978).

4. Behavioral Operating Characteristics And Vector Cell Properties In Precentral Motor Cortex

Because the VITE model proposes that trajectories are generated as the arm tracks the evolving state of a neural circuit's output stage (the PPC), the model can be tested in two ways: by comparing trajectories of the neural circuit's output stage (e.g., Figures 3,4) with behavioral data concerning actual arm trajectories, and by checking for the existence of the neural components postulated in the model. Detailed quantitative comparisons of model predictions with behavioral data can be found in Bullock and Grossberg (1988a, 1988b). Among the properties treated therein are: Woodworth's distance-error law (Woodworth, 1899); the speed-accuracy trade-off known as Fitts' law (Fitts, 1954); peak acceleration as a function of movement amplitude and duration, and isotonic arm movement properties before and after arm-deafferentation in animals deprived of visual feedback (Bizzi, Accornero, Chapple, & Hogan, 1984); synchronous and compensatory "central error correction" properties of isometric contractions (Gordon & Ghez, 1987); velocity amplification during target switching (Figure 7 and Georgopoulos, Kalaska, & Massey, 1981); velocity profile invariance across different movement distances (Figure 3A,B and Freund & Büdingen, 1978) and change in profile asymmetry across different movement durations (Figure 3C-F and Beggs & Howarth, 1972; Moore and Marteniuk, 1986; Zelaznik, Schmidt, and Gielen, 1986); and changes in the ratio of maximum to average velocity during discrete vs serial movements (Ostry, Cooke, & Munhall, 1987).

Neurophysiological data support the existence of the major stages in the VITE model. In particular, the VITE model includes a DV stage, the analogue of which does not exist within mass-spring models of trajectory formation (e.g., Cooke, 1980). Cell populations have been identified that possess all the properties required of an *in vivo* analogue of DV stage neurons. For example, Georgopoulos and associates (Georgopoulos, Kalaska, Caminiti, & Massey, 1984; Schwartz, Kettner, and Georgopoulos, 1988) have located a class of cells in the shoulder-elbow zone of the precentral motor cortex (Area 4). Called vector cells, they have the following properties in common with VITE model DV cells: (1) activity levels correlate with arm movement direction but not arm movement endpoint; (2) activity levels may be primed prior to movement, as required by the postulate that actual movement depends on GO signal activation; (3) the time course of vector cells is highly correlated with the time course of the model DV; (4) vector cell coding of movement

direction does not reverse during the second half of the movement, indicating pure kinematic coding with no braking-force component, consistent with the VITE-FLETE-MLN parsing strategy; and (5) vector cells project to interneurons rather than directly to motoneurons, as required by the VITE model postulate of an outflow PPC stage that must be supplemented by FLETE and MLN signals to generate the total movement command. Thus the VITE model provides a mechanistic understanding of how the neural population vectors measured by Georgopoulos and associates may be computed by a distributed neural circuit (for further details, see Bullock & Grossberg, 1988a; Georgopoulos, this volume).

5. Physiological Evidence For Globus Pallidus As A Component Of The GO Signal Pathway

In addition to evidence of Georgopoulos and his colleagues that cell populations in precentral motor cortex behave like an *in vivo* analogue of model DV stage neurons, physiological support for the VITE model comes from recent experiments involving lesions, electrical stimulation and microelectrode recording studies of the basal ganglia. Data from a set of experiments by Horak and Anderson (1984a, 1984b; Anderson & Horak, 1985) are consistent with the interpretation that the internal segment of the globus pallidus is a component of an *in vivo* analogue of the VITE model's GO signal pathway.

An *in vivo* candidate for a GO signal pathway must pass four tests. First, stimulation at some site in the proposed pathway must have an effect on the rate of muscle contractions. Second, it must have this effect without affecting the amplitude of the contractions. Thus stimulation should have no effect on movement accuracy, except possibly for effects caused by imperfect motor realization of the PPC commands. Third, this rate-modulating effect should be non-specific: it should affect all muscles that are typically synergists for the movement in question. Fourth, because movement depends on the conjunction of a positive DV and a positive GO signal (Equation 3), no movement should occur in the absence of either signal.

The studies conducted by Horak and Anderson (1984a, 1984b) pertain to all of these issues. Horak and Anderson (1984a) showed that "when neurons in the globus pallidus [of Macaque monkeys] were destroyed by injections of kainic acid (KA) during task execution, contralateral arm movement times (MT) were increased significantly, with

little or no change in reaction times" (p.290). This satisfies the *rate criterion*. Moreover, the rate of motor recruitment was depressed "in all the contralateral muscles studied at the wrist, elbow, shoulder, and back, but there were no changes in the sequential activation of the muscles" (p.20). This satisfies the *non-specificity criterion*. Finally, the authors also noted that "animals displayed no obvious difficulty in aiming accurately... they did not miss the 1.5-cm target more often following KA injections, and there was no noticeable dysmetria around the target" (p.300). This satisfies the *accuracy criterion*.

Horak and Anderson (1984b) used an electrical stimulation paradigm instead of a lesion paradigm. They found that "stimulation in the ventrolateral internal segment of the globus pallidus (GP_i) or in the ansa lenticularis reduced movement time, whereas stimulation at many sites in the external pallidal segment (GP_e), dorsal GP_i, and putamen increased movement times for the contralateral arm" (p.305). Once again, these effects were non-specific: "no somatotopic effects of stimulation were evident. If stimulation at a site produced slowing, it produced a depression of activity in all the muscles studied. Even stimulus currents as low as 25 μA affected proximal as well as distal muscles, flexor as well as extensor muscles, and early–as well as late–occurring activity" (p.309).

The *conjunction criterion* for a GO-signal pathway was also met. In the VITE model, activation of the GO-signal pathway produces movement only if instatement of a TPC different from the current PPC leads to the computation of a non-zero DV, regardless of the value of $G(t)$. In agreement with this property, Horak and Anderson (1984b) observed that "stimulation at sites that speeded movements did not induce involuntary muscle activation in resting animals nor did it change background EMG activity prior to self-generated activity during task performance" (p.313). In Bullock and Grossberg (1988a) we noted that "very rapid freezing can be achieved by *completely* inhibiting the GO signal at any point in the trajectory." This property of the model has been partially shown to be a property of the GP system by the demonstration that stimulation in inhibitory zones adjacent to GP_i significantly slowed movement, as noted above. Interestingly, Horak and Anderson also reported that "stimulation with 50 or 100 μA at...sites ventral and medial to typical GP_i neuronal activity completely and immediately halted the monkey's performance in the task" (p.315). Though the sites producing halting in the Horak and Anderson studies apparently do not inhibit the GP_i, they may inhibit targets of the GP_i output pathway. Prior studies using much larger currents in zones known to inhibit GP_i have produced halting (Van

Buren, Li, & Ojemann, 1966). Taken together, their experiments led Horak and Anderson (1984b) to conclude that "the basal ganglia...determine the speed of the movement" (p.321). Consistent rate-control data for speech movements have been reported by Mateer (1978).

In a study of timing relations between natural pallidal neuron discharges and the earliest detectable EMG activity, Anderson and Horak (1985) observed that though about 30% of pallidal neurons began firing 50-150 ms before mechanically detectable movement, "only 13 of 108 neurons showed changes in activity before the earliest EMG activity recorded during the same trials, and for only two of them did the initial changes in firing rate precede the initial changes in EMG activity by more than 25 ms" (p. 444). From this they conclude that "it is unlikely that changes in pallidal firing would be important in determining the initiation of the arm movement... but they could be important in controlling the buildup or scaling of EMG activity and thus the duration of the movement" (p. 444). Similar timing relations in monkeys have been reported by Mitchell, Richardson, Baker, and DeLong (1987).

These timing relations have several alternative interpretations that require further discussion, especially in the light of cat data consistent with an initiating role for pallidal output signals (Neafsey, Hull, & Buchwald, 1978). Before beginning our discussion, we note that even if we accepted Anderson and Horak's caveat regarding initiation, the GP would still be implicated in GO-signal buildup, but in such a way that the GO signal can begin its gating action before the pallidal part of the circuit becomes engaged. Such a picture is consistent with one aspect of the proposal of Penney and Young (1983), that the globus pallidus is part of a positive feedback loop, which could be used to help generate a GO signal that grows in time with the shape shown in Figure 3.

However, both theoretical and empirical considerations suggest that Anderson and Horak may have underestimated the role of the GP_i in movement initiation. In any planned movement context, there are likely to be a set of central events, all of which may be jointly involved in "determining the initiation of the arm movement." In particular, an arm movement will be more successful if the muscles controlling body segments that serve as the postural base for the arm are activated before the phasic arm movement is itself initiated. Gahery and Massion (1985) have reported central and muscular postural adjustments with lead times in excess of 25 msec before the onset times for central and muscular arm-movement producing activations.

From this perspective, the data of Anderson and Horak do not rule out the GP_i as a GO signal generator. Rather, they further buttress the argument that a gradually increasing GO signal exists in the GP_i . In particular, each animal individually showed some pallidal activity at least 25 msec prior to the earliest EMG activity. Inspection of Anderson and Horak's (1985) Figure 8 reveals that this "short" 25 msec lead time held only for the thoracic paraspinal muscle, whose activity was probably generated by the separate circuit responsible for preparing the postural base for the forthcoming arm movement (Gahery & Massion, 1985). In contrast, pallidal activity led EMG activity in all arm-projection muscles (biceps, deltoid, radialis) by at least 50 ms. Such a lead time is compatible with an initiating role because the GP_i may be tri-synaptically linked to motoneurons via two separate pathways.

In addition, Anderson and Horak used a simple RT task, which allows complete DV priming. Such a task would be expected to eliminate any effect of the GO signal on RT as well as reduce to a minimum the lag between GO activation and initial muscle activation. Initial muscle activity is affected by the product of the GO signal and the large initial DV. Because the GO signal is assumed to start small and to grow gradually, only a small proportion of pallidal neurons should become active prior to initial muscle activity. Thus the Anderson and Horak (1985) observations of gradual recruitment of active pallidal neurons are consistent with the model postulate of a gradually growing GO signal (Figure 3). The hypothesis of a gradually growing GO signal was needed to quantitatively explain parametric data about arm movement velocity profiles (Bullock & Grossberg, 1988a).

The internal segment of the globus pallidus is one of two main output nuclei for the basal ganglia (BG). An assessment of its role as a GO signal generator thus needs to consider inputs to the basal ganglia. In particular, it is necessary to ask whether the basal ganglia receive the afferents one would expect to govern the final decision to execute a primed motor command. This issue has recently been addressed by Passingham (1987), who concluded "that it is the basal ganglia that finally direct the action to be taken" (p.90). Regarding BG inputs, he noted that for a correct evaluation of the context for action, "the motor system must be influenced by information from all of the cortical regions....In fact there is a massive projection from all these areas, but it runs not across the cortex but downward to the basal ganglia" (p.85). Moreover "the ventral striatum [one of the BG input zones] receives a heavy projection from the amygdala...[which] plays a crucial role in the learning of

motivational and emotional associations" (p.85). Thus the basal ganglia receive inputs whereby cognitive and motivational information may be integrated to arrive at decisions to act.

The other main output nucleus of the basal ganglia--the substantia nigra (SN) pars reticulata--is known to gate read-out of movement commands controlling saccadic eye movements. It does this by disinhibiting deeper layers of the superior colliculus (Sparks & Jay, 1986; Wurtz and Hikosaka, 1986). Grossberg and Kuperstein (1986, 1989) have modelled how this gating action enables planned and attentionally modulated eye movement commands to effectively compete with more rapidly computed visually reactive eye movement commands to decide which type of information will determine where the eye looks in any given situation. In baboons, SN lesions produced a marked increase in the duration of a forelimb pointing movement without causing a change in movement accuracy, and the slowing involved the whole trajectory (Viallet, Trouche, Beaubaton, Nieoullon, & Legallet, 1983), consistent with Equation (2).

6. Target Switching During Movement Sequences

By supporting VITE model predictions regarding separate DV and GO signal processes, the data of Georgopoulos et al. and Horak and Anderson also support the more general hypothesis that motor systems, like sensory systems, implement factorization of pattern and energy (Section 1). In the VITE component, this factorization means that a movement's speed ("energy") can be scaled up or down over a wide range without disrupting the movement's direction or spatial endpoint ("pattern"). By using a GO signal that grows gradually during the movement time (Figure 3), all synergists complete their contractions at approximately the same time even if movement onset times of different synergists are staggered by a large amount (Figure 4). These properties of the model, together with the strong evidence for separate DV and GO signal pathways *in vivo*, provide a basis for understanding how primates can achieve space-time equifinality--all synergists reaching their length targets at equal times--yet retain separate control of rate and position. Rate-control models relying on *static* stiffness adjustments (e.g., Cooke, 1980) lack this critical temporal-equifinality property.

A closely related property of the VITE model gains importance during the many occasions when the TPC is updated one or more times during a movement or movement sequence. This may occur, for example,

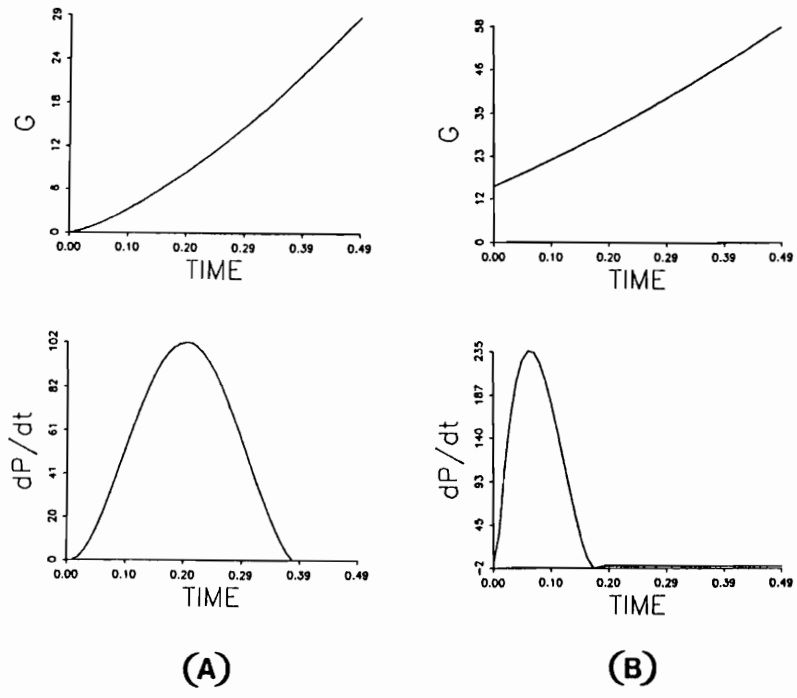

Figure 7. A much higher peak velocity is predicted by the model whenever a target, T, is activated after the GO signal has already had time to grow. (A): The control condition, in which T and the GO-signal growth process are activated synchronously. (B): Same T as in (A), but here T was activated after the GO signal $G(t)$ had been growing for 300 ms.

if the position of the object to be reached unexpectedly changes. Alternatively, a subject reaching for an object that is initially in the visual periphery may make a better estimate of object location after performing a saccadic eye movement to foveate the object. Saccades take less time than an arm movement that may be unfolding in parallel. In either case, the TPC and DV are rapidly updated, and this late-arriving information affects the arm's trajectory more quickly because the GO signal is already fully developed. Thus the factorization of TPC and GO signal, along with the hypothesis of a gradually growing GO signal, implies that a higher peak velocity will be achieved as a result of a mid-trajectory switch in TPC (Figure 7). Such an amplification of velocity facilitates reaching the target after the incorrect initial TPC is updated. This speed-up occurs "on-the-fly" as the effects of the perturbation flow through the system via

dynamic real-time computations. Georgopoulos et al. (1981) have reported such an increase of peak velocity during target-switching experiments in monkeys.

An experiment by Goodale, Pelisson, and Prablanc (1986), analogous to the Georgopoulos et al. (1981) study with monkeys, showed that humans also possess the ability to compensate for in-course target switches. Their experiment was also consistent with an explanation in terms of TPC updating and flow-through, because they eliminated the possibility that corrections could be based on visual comparisons of the relative positions of hand and target. In particular, compensations to a change in target position occurred in the arm's trajectory even when the arm and hand were invisible to the subject.

Fisk and Goodale (1988) have offered an interpretation of late-occurring in-course error corrections, also proposed by Cooke and Diggles (1984), that is consistent with VITE model mechanisms. They concluded that many terminal error corrections are not based on either proprioceptive feedback from the limb or on visual comparisons of the relative positions of hand and target. Rather, such corrections are based on a comparison made between an internal representation of the target's locus and an internal representation of the hand's estimated location based on movement commands. These results support the VITE model as well as the classical hypothesis that even infants typically perform reaches without needing to compare the position of their seen hand with the seen target (Piaget, 1963).

7. From Kinematics To Dynamics: Generating Forces To Ensure That The Arm Tracks The Evolving PPC

The VITE circuit places stringent requirements on other components of the sensory-motor system because it requires continuous or near-continuous adjustment of the balance of forces acting on the limb to ensure that the limb tracks the evolving PPC without significant lags or overshoots. Some of these components are modelled herein to explain how they autonomously generate the force-time patterns required to track VITE-generated trajectories. When both types of circuits are understood, a quantitative mechanistic understanding of two of the most fundamental problems in sensory-guided motor control would then be approached: how to generate continuously modifiable kinematic plans, and how to generate the continuously modifiable force-time patterns needed to realize them.

8. Factorization Of Length And Tension (FLETE) Model

A critical step toward a coherent theory of force-time pattern generation is a principled explanation of the basic spinal-motor-receptor architecture that exists across species. Modelling and computer simulations of this system (Figure 8) suggest that all the major components of the basic architecture play a role in guaranteeing that force (muscle tension) and position (muscle length) are independently controllable by descending control signals of a few simple types. To emphasize this model's central claim of **F**actorization of **LE**ngth and **TE**nsion, the model is called the FLETE model. The next sections describe some results that were reported in preliminary form in Bullock and Grossberg (1988d).

Past research in this direction has focused on muscle operating characteristics and the alpha-gamma subsystem. An excellent recent fusion of these two traditions can be found in Gielen and Houk (1987), which shows that muscles, receptors, and alpha-gamma circuits can together act as a length servo at low speeds and a velocity servo at high speeds. However, several aspects of the basic system have remained obscure, such as the role of the recurrent inhibition mediated by Renshaw cells, and the contribution of the size principle of motor neuron recruitment. Many recent treatments of Renshaw inhibition relegate it to the role of controlling the gain of the stretch reflex (e.g., McMahon, 1984). FLETE simulations indicate that viewing the Renshaw → MN and Renshaw → Ia → MN circuits (Figure 8) as merely an "epicycle" to the alpha-gamma circuit is insufficient, and suggest a revised functional basis for the size principle of motor neuron recruitment. A summary of both results follows.

9. Wide Force Range At Each Fixed Muscle Length Requires Size Principle

By Newtonian mechanics, the position of a limb is controlled by the balance of forces acting on it. In the body, muscles are the force generators by which this balance is controlled. Muscle is a springy tissue that can actively contract. In a spring, the amount of force depends on the amount of stretch beyond the resting length, the threshold-length for force development. Because muscle can actively contract, muscle has a *variable* threshold-length for force development. The basic spring-like

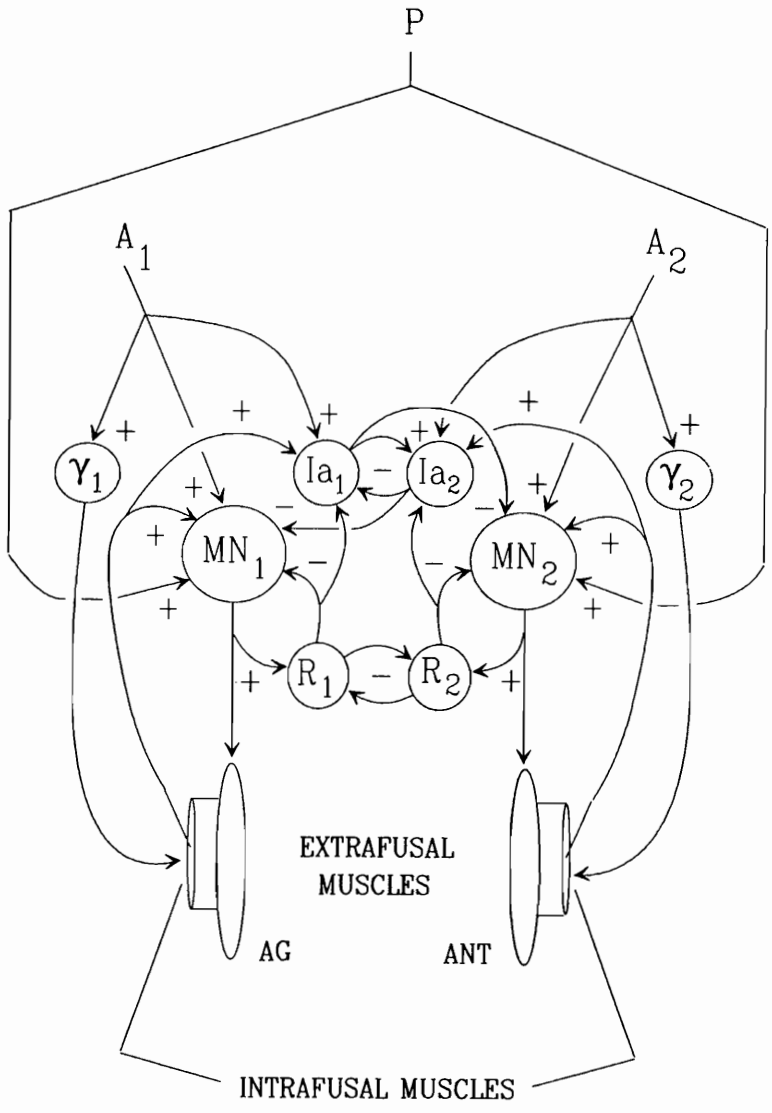

Figure 8. Components of the FLETE model of the peripheral skeleto-motor system. Neuron populations comprising two channels together control the contractile states of opponent muscles (AG for agonist, ANT for antagonist) acting on a joint. Descending signal P to both channels allows co-contraction and joint stiffening. Adjusting the balance between descending signals A_1 and A_2 allows reciprocal contractions and joint repositioning. For clarity, subpopulations of neurons and some signal pathways are not depicted. Key: Ia_i = Ia interneuron population in channel i, i = 1,2; γ_i = gamma motoneurons; MN_i = alpha motoneurons; R_i = Renshaw cells; + = excitatory input; − = inhibitory input.

property can be approximated by the equation

$$F = g([\mathrm{L} - \Gamma]^+) \tag{7}$$

where F is force, L is muscle length, Γ is a threshold length, g is a monotone increasing function, and notation

$$[\omega]^+ = \begin{cases} \omega \text{ if } \omega > 0 \\ 0 \text{ if } \omega \leq 0. \end{cases} \tag{8}$$

Because active contraction can lower the threshold, (8) is replaced by

$$F = g([L - (\Gamma - C)]^+) \tag{9}$$

or equivalently

$$F = g([L - \Gamma + C]^+), \tag{10}$$

where C measures the amount of contraction. Note that active contraction does not result in muscle shortening if another force--such as that developed by an opponent muscle--counteracts the contractive force. For the subsequent discussion it is very important to remember that muscles often actively contract without changing their length, as measured from origin to insertion.

Suppose that two opponent muscles exert forces F_1 and F_2 from opposite sides of a rotating limb segment (Figure 9) and that the outputs from antagonistic PPC stages in a VITE circuit (Figure 2) are sent to a stage capable of directly adjusting C_1 and C_2 in the following equations for F_1 and F_2:

$$F_1 = g([L_1 - \Gamma_1 + C_1]^+) \tag{11}$$

$$F_2 = g([L_2 - \Gamma_2 + C_2]^+), \tag{12}$$

where the Γ_i are constant thresholds.

If initially $F_1 = F_2$, then reducing C_1 and increasing C_2 by ΔC creates a force imbalance such that

$$F_2 > F_1 \tag{13}$$

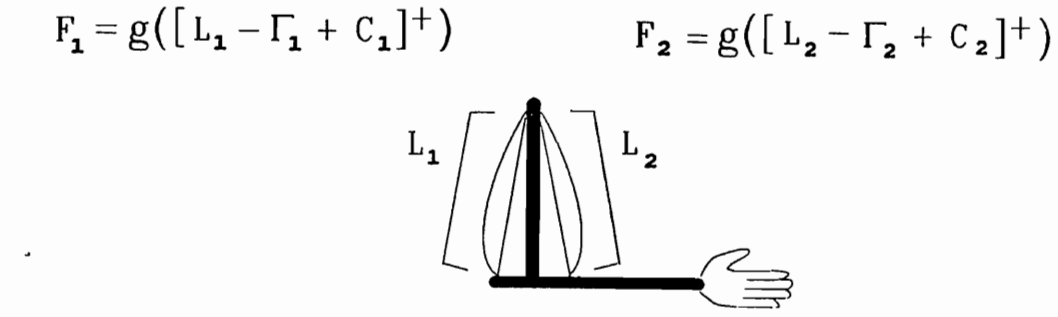

Figure 9. Equilibrium joint angle depends on the balance of forces developed by opponent muscles. Each muscle's force depends on its length L_i, its resting length Γ_i, and its active contractile state, C_i .

Rotation occurs until

$$[L_1 + \Delta L - \Gamma_1 + C_1 - \Delta C]^+ = [L_2 - \Delta L - \Gamma_2 + C_2 + \Delta C]^+ \quad (14)$$

and a force balance is once again restored.

In vivo, the alpha-motoneurons transiently activate contractile fibers from a finite population of fibers. As in equations (11) and (12), let C_i be the degree of contraction, and let M_i be the output signal of the motoneuron pool in channel i, $i = 1,2$. Then a simple law for change in contraction in a finite population is:

$$\frac{d}{dt} C_i = (B_i - C_i)M_i - \delta C_i . \quad (15)$$

This says that M_i increases C_i by activating unactivated fibers, which number $(B_i - C_i)$, from a population of size B_i, and that contraction spontaneously decays at rate δ.

However, it is known that contracted fibers yield, or decontract, when the force acting to stretch them is sufficiently large. Thus (15) is replaced by

$$\frac{d}{dt}\ C_i = \beta_i[(B_i - C_i)M_i - \delta C_i] - [F_i - \Gamma_F]^+ \tag{16}$$

where

$$0 < \beta_i < 1\ . \tag{17}$$

In equation (16), when the force exceeds the threshold level, Γ_F, it acts to reduce contraction. Inequality (17) acknowledges that any active contraction caused by neural input M_i is slow relative to the fast decontractive effect of suprathreshold forces.

The simple model (16) provides a new perspective for understanding the functional role of a widely observed, but imperfectly understood, physiological law. At equilibrium, $\frac{d}{dt}C_i = 0$ in (16), so that the equilibrium value of C_i is

$$C_i = \frac{M_iB_i - \frac{[F_i - \Gamma_F]^+}{\beta_i}}{M_i + \delta}\ . \tag{18}$$

Given (18), how is it possible to generate and sustain forces much larger than Γ_F at a *fixed muscle length*? Because

$$F_i = g([L_i - \Gamma_i + C_i]^+) \tag{19}$$

in (11) and (12), where Γ_i is a constant, greater force at a fixed length L_i can be generated only by increasing C_i . However, if β_i is constant and less than 1, then (18) shows that the negative force feedback will cancel the effects of increasing M_i, and C_i will not be able to increase, at least if a near linear or faster-than-linear $g(\omega)$ is assumed.

To overcome this deficiency within the constraints imposed by equation (16), let the contraction rate parameter β_i and the number of sites B_i increase with M_i . Such a relation is well documented empirically and is often called "Henneman's size principle" (Henneman, 1957; 1985): As total excitatory input to the alpha motoneuron population grows, it recruits additional, progressively larger motoneurons which have faster

conducting axons, whose collaterals reach many more motor fibers and whose potentials evoke more rapid muscle contractions.

Prior treatments of the function of the size principle have focused on either the contraction-time effects or the force-magnitude effects seemingly implied by activation of cells that project to larger numbers of motor fibers. The present analysis suggests that both aspects of the size principle help realize a large force range at any fixed muscle length. In particular, merely making B_i increase with M_i is not enough. The contraction rate parameter β_i also needs to increase with M_i . Thus contractile rate is as critical a component of the system for yielding compensation as the more frequently cited reflex circuits (Houk & Rymer, 1981).

Assuming that $g(\omega)$ is slightly faster than linear, e.g.,

$$g(\omega) = \omega^{\alpha}, \quad 1< \alpha <2 , \tag{20}$$

then the system

$$F_i = ([L_i - \Gamma_i + C_i]^+)^{\alpha} \tag{21}$$

$$\frac{d}{dt} C_i = \beta_i[(B_i - C_i)M_i - \delta C_i] - [F_i - \Gamma_F]^+. \tag{16}$$

generates a family of curves like those shown in Figure 10 where equilibrium force is plotted as a function of muscle length for four different values of M_i with β_i and B_i constant. Data from experiments in which equilibrium muscle tension (in areflexive muscle) was measured as a function of length and frequency of electrical stimulation have the same form with one difference: the higher stimulation rates lead to slightly larger slopes and higher asymptotic tensions (Rack & Westbury, 1969). From the above analysis, both the slope change and the raised peak tension can be attributed to the size principle: higher stimulation rates evoke faster-contracting fibers, which leads to a higher equilibrium C_i and F_i, and a higher multiplier of L_i .

10. Size Principle With Co-Contraction Poses A Threat To Invariant Position Coding

The above analysis suggests that the size principle plays a major role in generating a wide range of forces at each fixed muscle length. This

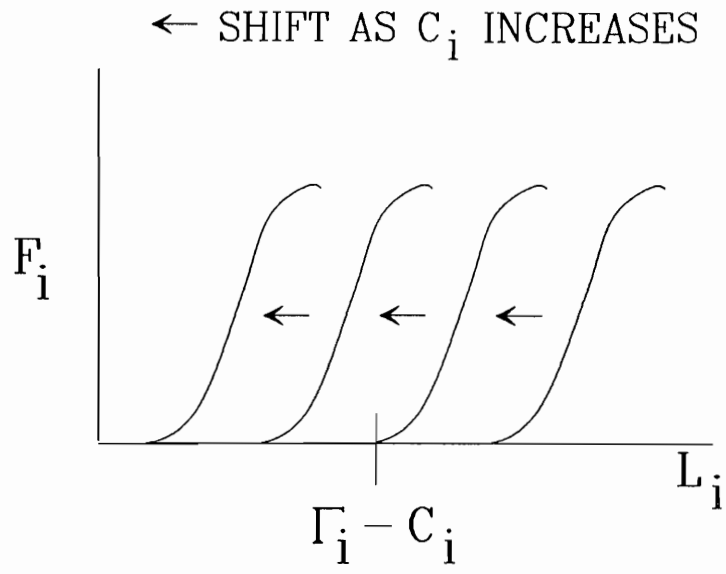

Figure 10. In first approximation, the effect of increased muscle stimulation is a shift in the threshold length for force development.

property is important both during high co-contraction conditions when the arm resists changes in position due to variable external forces (e.g., Humphrey & Reed, 1983), and in carrying out planned arm movements wherein the arm undergoes a continuous change of position. In the latter situation, the ability to generate a wide range of forces at each position of a movement trajectory is needed to enable the arm to accurately track the PPC commands that are continuously read-out at variable rates by central circuits. During trajectory formation, a wide range is also needed to compensate for variable forces due either to external perturbations of the arm or to variable arm inertias caused by variable velocities or trajectories of variable shape (e.g., Lestienne, 1979).

However, we now show that the size principle, while extending the force range, can also pose a threat to invariant position coding. In particular, we describe an example that shows how the size principle could prevent *any* simple PPC code from being realized by the arm, such as one based upon adjusting the relative sizes of PPC commands to agonist-antagonist muscle groups. We then present the additional neural circuit needed to negate this threat.

As illustration of the invariance problem, suppose that a limb segment is initially at equilibrium, such that

$$F_1 = F_2 \,. \tag{22}$$

By (19),

$$g([L_1 - \Gamma_1 + C_1(A_1)]^+) = g([L_2 - \Gamma_2 + C_2(A_2)]^+), \tag{23}$$

where $C_1(A_1)$ denotes the equilibrium value of C_1 when $M_1 = f(A_1)$ in (16). Now suppose that we attempt to hold the limb at the same position, but more rigidly, by increasing the level of muscle contraction on both sides of the joint. The simplest way to do this is by adding a constant, P, to each motoneuron input. Thus $M_1 = f(A_1+P)$ and $M_2 = f(A_2+P)$. However, in a system that obeys the size principle, equation (23) implies

$$g([L_1 - \Gamma_1 + C_1(A_1 + P)]^+) = g([L_2 - \Gamma_2 + C_2(A_2 + P)]^+) \tag{24}$$

for arbitrary values of P and the same initial values of L_i only if $A_1 = A_2$ (see explanation in Figure 11). In other words, sending the same co-contractive input P to both motoneuron pools in an attempt to further stabilize current limb position could instead cause a limb rotation. This is a prime example of a failure of factorization of length and tension: an attempt to change only tension inadvertently changes length. Because the motor cortex appears to follow the simplest strategy (adding a constant P; see section 14), some mechanism must exist to prevent unwanted limb rotations.

In the light of this problem, many researchers have proposed that C_i and L_i should interact multiplicatively to produce force. Though this would reduce the problem, the proposal amounts to a claim that the primary effect of changing M_i is a change in the stiffness ($\Delta F/\Delta L$) of areflexive (deafferented) muscle. However, experimental data show that stiffness changes relatively little as M_i changes; the primary effect of changing M_i is a change in the threshold length for force development, as suggested in Equation (9) and Figure 10 (Feldman, 1986; Rack & Westbury, 1969).

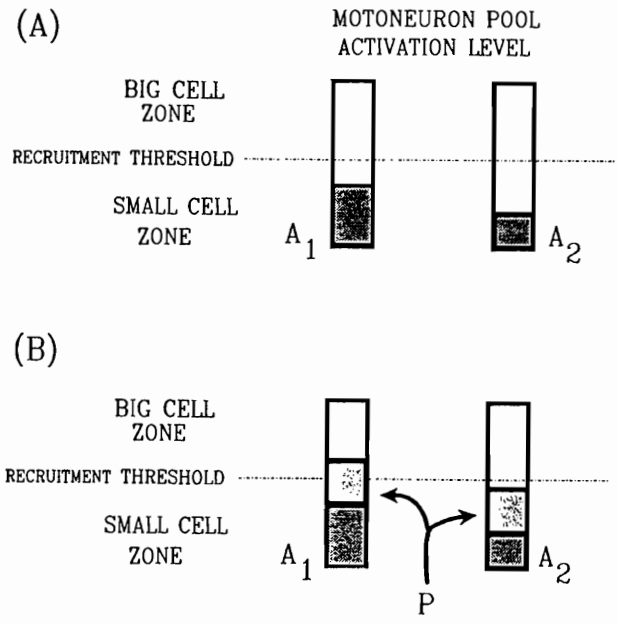

Figure 11. When opponent motoneuron populations obey the size principle, a co-contractive signal P sent in parallel to both populations can disrupt the joint position code. (A) Signals A_1 and A_2 supraliminally activate only small cells in opposing channels and their relative sizes determine the balance of muscular forces and thus the equilibrium joint position. (B) With $A_1 > A_2$, co-contractive signal P causes the total input $A_1 + P$ to exceed the big cell threshold while input $A_2 + P$ remains below the big cell threshold. Thus part of the signal P is subjected to greater amplification in channel 1 than in channel 2. Unless compensated, this would create a new balance of forces and cause an unwanted joint rotation.

11. Compensatory Properties Of Renshaw-Ia Pathway

An alternative solution may be sought in known neural circuits. Is there any neural site that is sensitive to the amplification factor (Figure 11) introduced by progressive recruitment within an alpha-motoneuron population? The alpha-gamma system cannot provide the type of compensation desired because gamma motoneurons are not sensitive to the amplification. However, inspection of Figure 8 reveals the Renshaw cells as sole neural targets of α-MN axon collaterals, and that α-MN cells receive feedback signals from Renshaw cells. Thus Renshaw cells are well situated to measure and modify the final output of the motor channel. Moreover, it is known that collaterals of larger, later recruited motoneurons make many more synaptic contacts with Renshaw cells than smaller, earlier recruited motoneurons (Cullheim and Kellerth, 1978). These properties are consistent with the hypothesis that Renshaw cells

play the required compensatory role. We now present computer simulations of the system in Figure 8 which show how model Renshaw cells can compensate for position code distortions that would otherwise be generated when co-contraction is combined with the size principle of motoneuron recruitment. This property depends upon how the feedback pathways in the circuit are organized into opponent, or antagonistic, muscle channels.

Table 1
Major FLETE Model Variables

A_i	Descending reciprocal input to alpha motoneuron and Ia interneuron population i, $i = 1,2$
P	Descending co-contractive input to both alpha motoneuron populations
F_i	Force developed by muscle i, $i = 1,2$
C_i	Contractile state of muscle i, $i = 1,2$
L_i	Origin-to-insertion length of muscle i, $i = 1,2$
M_i	Alpha-MN population activity, $i = 1,2$
R_i	Renshaw population activity, $i = 1,2$
I_i	IaIN population activity, $i = 1,2$
E_i	Composite signal from spindle organs, $i = 1,2$

The compensation occurs as follows. Opponent Renshaw populations R_1 and R_2 measure the output of their respective alpha-motoneuron populations, α-MN_1, and α-MN_2, and compare those outputs via mutually inhibitory signals (Figure 8). A consensus emerges regarding which MN channel to inhibit via Renshaw feedback, and which to disinhibit via feedback from the Ia interneuron (IaIN) pathway. Suppose that a co-contractive input, P, to α-MN_1 and α-MN_2 occurs when input A_1 exceeds A_2. Suppose that the activity of α-MN_1 is consequently multiplied by a larger factor than that of α-MN_2 due to the size principle (Figure 11). Then R_1 also becomes much more active due to the size-correlated synaptic weighting on α-MN_1 axon collaterals to R_1. Because the opposing R_2 has not experienced as large an input increment, R_1 will transiently become more active than R_2 by an amount that scales with the

difference between the α-MN output increments due to the change in P. Thus this system calculates an *error* due to unequal amplifications of co-contractive inputs. This error signal then directly inhibits α-MN_1 and, by inhibiting $IaIN_1$, indirectly activates α-MN_2. Both actions work to zero the error without negating either the shared increment in α-MN_i activation required to increase joint stiffness, or the joint angle setting determined by the difference in descending inputs, exclusive of P, to opponent α-MN and IaIN populations.

Readers not interested in the details of the simulations should skip ahead to the *Results* subheading. Others may consult Table 1 for definitions relevant to equations (25)-(37).

As in Figure 9, we assumed a rotary joint affected by two opponent muscles, each of which is inserted in the moving segment one unit from the axis of rotation. The distance from muscle origin to the axis of rotation was 20 units, and the midpoint of the limb's 180° excursion was stipulated to be at joint angle $\Theta = 0°$. Origin-to-insertion muscle lengths, L_i, were thus functions of Θ:

$$L_1 = \sqrt{(\cos\Theta)^2 + (20 - \sin\Theta)^2} \tag{25}$$

$$L_2 = \sqrt{(\cos\Theta)^2 + (20 + \sin\Theta)^2} \tag{26}$$

In the simulations reported here, we were interested only in large-scale effects on equilibrium joint angle. Thus we ignored moment-arm and force-velocity effects and chose the simple force law

$$F_i = k[L_i - \Gamma_i + C_i]^+ \tag{27}$$

where $k = .5$, $\Gamma_i = 20.9$ and $i = 1,2$. Limb dynamics were governed by equation

$$\frac{d^2}{dt^2}\Theta = \frac{1}{m}\left(F_1 - F_2 - n\frac{d\Theta}{dt}\right) \tag{28}$$

where m represents mass and n is a damping coefficient. Contractile state C_i was governed by

$$\frac{d}{dt}C_i = \beta_i[(B_i - C_i)M_i - \delta C_i] - [F_i - \Gamma_F]^+. \tag{16}$$

with $\delta = 1$, and $\Gamma_F = 0$. Variables β_i and B_i were defined by:

$$\beta_i = .05 + .02(A_i + P) \tag{29}$$

$$B_i = 2 + 20(A_i + P) \tag{30}$$

Both variables grow as a function of total descending input A_i+P to the MN pools in channel i, but β_i grows with a smaller slope.

Equations (16), (29), and (30) use parameters β_i and B_i to approximate α-MN recruitment effects that occur *in vivo*. Which α-MNs exceed threshold may depend not only on the total descending drive, A_i+P, as in (29) and (30), but also on inhibitory inputs from IaINs and Renshaw cells as well as on inputs arising from sensory organs in the muscle. In this lumped model, sensory feedback was omitted to isolate the potential compensatory effect of the Renshaw pathway.

The lumped model does, however, include the critical assumptions that Renshaw populations associated with opponent muscles are mutually inhibitory, and that each Renshaw populations's activity be sensitive to the amplification factor introduced by recruitment of larger motoneurons. Such sensitivity requires that growth in a Renshaw population's activity not saturate prior to saturation of growth in α-MN population activity, and that the input to the Renshaw population scale with the net amplification due to recruitment. As noted above, there is evidence that this scaling is effected in vivo by increasing the synaptic weighting factor associated with Renshaw-directed axon collaterals from larger α-MNs. In our lumped model, this effect was absorbed into a single variable coefficient, z_i, which was made a function of recruitment extent, as approximated by A_i+P. The lumped equations for opponent Renshaw populations were thus

$$\frac{d}{dt} R_1 = (\lambda B_1 - R_1) z_1 M_1 - R_1(1 + R_2) \tag{31}$$

$$\frac{d}{dt} R_2 = (\lambda B_2 - R_2) z_2 M_2 - R_2(1 + R_1) \tag{32}$$

with $\lambda = 5$ and

$$z_i = .2 + .8\ (A_i+P) \tag{33}$$

for $i = 1,2$. Parameter B_i in (31) and (32) approximates the property that the Renshaw population has a continuum of recruitment thresholds similar to the α-MN population, and that the number of suprathreshold Renshaw sites increases as more α-MNs are recruited (with increasing A_i+P).

We modeled the opponent alpha-motoneuron populations via

$$\frac{d}{dt} M_1 = \phi[(\lambda B_1 - M_1)(A_1 + P + \chi E_1)] - M_1(1 + \Omega R_1 + I_2) \quad (34)$$

$$\frac{d}{dt} M_2 = \phi[(\lambda B_2 - M_2)(A_2 + P + \chi E_2)] - M_2(1 + \Omega R_2 + I_1) \quad (35)$$

where $\phi = .2$, $\chi = 0$, and $\Omega = 0$ or 1. The inhibitory I_i inputs represent signals from the IaINs (see Figure 8) and the excitatory E_1 inputs represent signals from the muscle spindles.

We assumed that IaINs were not subject to any recruitment effects. Thus their dynamics were modeled without a direct dependence on B_i, and without a co-activating input P:

$$\frac{d}{dt} I_1 = \phi(10 - I_1)(A_1 + \chi E_1) - I_1(1 + \Omega R_1 + I_2) \quad (36)$$

$$\frac{d}{dt} I_2 = \phi(10 - I_2)(A_2 + \chi E_2) - I_2(1 + \Omega R_2 + I_1) \quad (37)$$

Composite spindle feedback signals E_1 and E_2 (in Equations 34-37) were gated off in our simulations by setting $\chi = 0$. This corresponds to destroying the stretch reflex via deafferentation, and it allowed us to test the ability of the Renshaw-Ia-MN feedback circuit to achieve position code invariance. The Renshaw feedback signals were gated on or off, respectively, by setting parameter Ω (in Equations 34-37) equal to 1 or 0.

Results

Table 2 shows representative numerical results. Variables A_1, A_2, and P (see Equation 24) represent constant inputs and variables L_1, F_1, and Θ represent equilibrium values of dependent variables. Because L_1 and L_2 are complements and $F_1 = F_2$ at equilibrium, L_2 and F_2 are omitted from the table. Because small length changes can imply large joint rotations, the most informative column in Table 2 is that showing

Θ, the equilibrium joint angle. When Renshaw feedback was absent ($\Omega = 0$), changing P while A_1 and A_2 remained fixed led to large undesirable rotations (10° in block 1, 22° in block 3). However when Renshaw feedback was present ($\Omega = 1$), rotations due to changing P with fixed A_1 and A_2 were extremely small (<1° in block 2 and <4° in block 4). Generally, when the system was not forced to operate in the saturation range, excursions were <1° when Renshaw feedback was present.

Table 2
FLETE Model Simulations: Wide Force Range at Each Length and Independent Control of Force and Length When $\Omega = 1$

Ω	A_1	A_2	P	L_1	F_1	Θ
0	.12	.1	.0	19.82	0.02	11.6
0	.12	.1	.1	19.66	0.32	21.5
0	.12	.1	.8	19.70	7.8	18.8
1	.14	.1	.0	19.88	0.002	8.27
1	.14	.1	.1	19.87	0.13	9.16
1	.14	.1	.8	19.89	3.1	7.89
0	.14	.1	.0	19.58	0.04	26.0
0	.14	.1	.1	19.26	0.36	48.5
0	.14	.1	.8	19.37	7.9	39.9
1	.22	.1	.0	19.55	0.03	28.2
1	.22	.1	.1	19.54	0.19	28.9
1	.22	.1	.8	19.61	3.4	24.5

Because all stretch feedback was turned off in these simulations, this property of Renshaw feedback may not be described as "controlling the gain of the stretch reflex." Indeed, from the current perspective, the tonic stretch reflex mediated by type Ia and II feedback fibers from length-sensitive spindle organs might be viewed as a secondary system designed to compensate for residual errors left uncompensated by the Renshaw-Ia system. This impression is reinforced by data (Fromm, Haase & Wolf, 1977) indicating that type II fibers from spindles activate α-MN populations and inhibit Renshaw populations in their own outflow channel. This means that if Renshaw feedback is either too strong or too weak to fully correct cocontraction-related positioning errors, Renshaw feedback gain will be automatically adjusted in the correct direction by type II feedback from muscle spindles. This pathway would also help compensate for moment-arm effects not included in our simulations (see Hasan & Enoka, 1985).

12. Evidence For Assumed Distribution Of Renshaw Connectivity

Two critical hypotheses of our model are (a) that Renshaw cells participate in the size principle and (b) that the computational unit is the pair of opponent muscle channels.

A variety of evidence supports the hypothesis that Renshaw cells participate in the size principle. In the simulations that generated Table 2, this assumption was implemented by scaling up Renshaw population parameters in parallel with motor-unit rescaling as $A_i + P$ grows. Recent experiments surveyed by Pompeiano (1984) concur that "recurrent inhibition is produced mainly by large phasic neurons that are recruited late" (p. 526). In particular, Pompeiano and Wand (1976; Wand and Pompeiano, 1979) produced functional evidence for such a size-dependency, and Cullheim and Kellerth (1978) produced convergent anatomical evidence by showing that larger, phasic motoneurons make many more synaptic contacts with Renshaw cells than smaller, tonic motoneurons.

The second hypothesis has been well supported since Sherrington's (1906) observations of reciprocal inhibition, but is oddly ignored in many treatments. Our treatment extends the reciprocal inhibition principle, which is a "biggest competitor wins" principle at the IaIN stage (Figure 8), by including Renshaw populations which compete before supplying inhibitory feedback to the model's IaINs and alpha-motoneurons (Miller & Scott, 1977; Pompeiano, 1984). Because the channel with the larger

Renshaw activity receives more inhibition, reciprocal inhibition at the Renshaw stage follows a "biggest competitor loses" principle. This property extends the classical role of the Renshaws in stabilizing the peripheral skeleto-motor system; Renshaw inhibition works against extreme joint angle excursions and complements the intrinsic damping characteristics of muscles.

More generally (Figure 8), the FLETE model assumes that Renshaw cells have an inhibitory effect at three sites. The recurrent inhibition to the alpha-motoneuron population that excites them has long been well known (Renshaw, 1941; Eccles, Fatt, & Koketsu, 1954; see Pompeiano, 1984, for recent review). Inhibition of the IaIN population in the same outflow channel was demonstrated by Hultborn, Jankowska, and Lindstrom (1971) and confirmed by others (see Pompeiano, 1984, pp. 512-513). Renshaw inhibition of the Renshaw population of the opposing muscle channel, suspected since Renshaw (1946), has been convincingly demonstrated by Ryall (1970). Though there is also evidence that Renshaws have an inhibitory effect on gamma motoneurons (Pompeiano, 1984, pp. 509-511), the effect is known to be attenuated relative to that on alpha-MNs. Though nearly all alpha-MNs are inhibited by Renshaws, only about half of gamma-MNs are so inhibited, and in lesser degree.

The model also assumes that Renshaw cells are directly affected by an excitatory input from the alpha-motoneurons (see Renshaw, 1941), and an inhibitory input from the opposing-channel's Renshaw cells (noted above). The inhibitory stretch feedback noted earlier from spindle organs via group II fibers, which carry a length-correlated signal, will be incorporated in future simulations. In this connection, we note that a descending inhibitory input from the red nucleus to Renshaw populations is also well documented (Henatsch, Meyer-Lohman, Windhorst, & Schmidt, 1986). This inhibitory red nucleus output is coupled with another rubral output that excites alpha-motoneurons in the same outflow channel. Thus this descending rubral signal is analogous to the inflowing type II spindle signal. If this parallel rubral output is a reciprocal command (always increasing in one channel while decreasing in the opposing channel), it can be seen to be part of a feedforward adaptive gain control system (Grossberg & Kuperstein, 1986), which gradually learns to supply *predictively* the compensations the peripheral circuit can only supply *reactively* (see also Bullock, Carpenter, & Grossberg, 1989; Kawato, Furukawa, and Suzuki, 1987).

13. Prior Proposals Regarding Renshaw Function

Proposals regarding Renshaw function have evolved rapidly in recent years. Shepherd (1979) acknowledged that their function remained mysterious despite the long-standing hypothesis that they might serve as a source of surround inhibition (and thus perhaps to contrast enhance the motor-output signal). In the same year Hultborn et al. (1979) proposed that the Renshaws were well situated to control the gain of the alpha-motoneuron pool's response to excitatory inputs. This proposal was often restated in terms of controlling the gain of the stretch reflex (e.g., McMahon, 1984), a picture since reinforced by discovery of the descending (rubrospinal) pathways that both inhibit Renshaw cell activity (thus disinhibiting alpha-motoneurons) and excite alpha-motoneurons, resulting in a higher-gain stretch reflex (Henatsch et al., 1986) among other effects. The common scenario imagined for such Renshaw modulation was during muscle contraction intended to produce movement. Thus this consensus proposal is not in conflict with the present proposal, in which muscle contraction intended to prevent movement is seen to require that the Renshaw pathway not be inhibited by descending signals. Rather, our proposal can be seen as the logical complement to the consensus view, and as further evidence for the need to have mechanisms (Section 4) that automatically define active posture, active movement, and passive movement as distinct computational states.

A model by Miller and Scott (1977) shares our emphasis on competition between opponent Renshaw populations. However, the authors assumed that such competition implicated the Renshaw-Ia pathway in locomotor pattern generation, a different function than the one here proposed. Subsequent research (Pratt & Jordan, 1987) appears to have ruled out the possibility that the Renshaw-Ia pathway is part of a spinal locomotor generator.

Finally, though some aspects of our model are similar to Feldman's (1986) well known "λ" model of skeleto-motor control, neither of our descending control signals, A_i and P, correspond to Feldman's stretch-reflex parameter λ. Moreover, we believe that continued use of lumped parameters like λ, and a kindred overemphasis on the concept of stretch reflex, may hinder attempts to understand how the neuromuscular system is parsed into functional subsystems. A case in point is the discovery, upon unlumping reciprocal and co-contractive inputs, that the Renshaw-

Ia pathway may play a role far more interesting than being an epicycle of the stretch-reflex.

14. Physiological Evidence For Separate Cortical Control Of Non-Selective Co-Contractive Input To Motoneurons

FLETE model simulations of Renshaw function were based on the assumption that the co-contractive signal, P, is sent in parallel and without differential weighting to small and large MNs alike in both outflow channels (Figure 11). This hypothesis is supported by data of Humphrey and Reed (1983), who subjected monkeys to high-frequency, alternating-direction, torque perturbations at the wrist joint after they trained the monkeys to actively maintain their wrist angle within a small angular tolerance zone. To prevent the imposed torques from rotating their wrists to angles outside the desired range, monkeys instated high levels of tonic co-contraction in wrist flexors and extensors. Measurements of motor unit activity showed that high levels of co-contraction were achieved non-selectively and in accord with the size principle. In particular, Humphrey and Reed (1983) concluded that "As the speed of joint perturbation rises, the modulated [reciprocal] input to the MN pools is increased and a tonic coactivation signal is added....Thus, an explanation of our observed MN firing patterns requires no assumption of selectivity of descending inputs to motor units of different type, nor of any recruitment order different from that established in previous studies....Both [reciprocal and co-activating] control signals appear to converge on both fast and slow-twitch MNs" (p.366).

Humphrey and Reed (1983) were also able to identify a central source of co-activation signals. In Section 4, we cited evidence from Georgopoulos that precentral motor cortex (Area 4) served as a site of VITE-like DV computations and thus as a source of reciprocal commands received by spinal motor centers. Whereas Humphrey and Reed (1983) observed similar reciprocally-engaged precentral cells, they also discovered a new class of tonically active neurons they called S^{Δ} cells (S = steady, Δ = shift). These neurons, also found in precentral Area 4, predominated in a zone slightly anterior to the DV-like cells, and "when the animal voluntarily co-contracted his wrist muscles, as in stabilization of the wrist or tightening of a grip on the handle, these cells discharged in a brisk and tonic manner" (Humphrey & Reed, 1983, p.363). Moreover, microstimulation (12 to 20 μA) in the anterior, S^{Δ} cell, zone evoked a co-

activation of flexor and extensor muscles at the wrist and in some cases at other arm joints. Thus the primary motor cortex seems to be a source of both the specific (reciprocal) and the non-specific (co-contractive) signals assumed to ultimately converge on the spinal motoneurons in the FLETE model.

15. Tracking A Rapidly Changing PPC, And The Genesis Of Tri-Phasic EMG Bursts

Computer simulations have also been carried out of how the peripheral skeleto-motor system, as modelled by the FLETE equations, responds to a fast ramp input, similar in shape to the VITE circuit output in response to a large GO-signal. These simulations were directed at the question of whether a quickly changing *mono*tonic ramp input would lead to a *multi*phasic burst pattern at the alpha motoneuron stage of the model. *In vivo*, a so-called "tri-phasic" burst pattern is typically observed during fast movements (Lestienne, 1979). If such a triphasic pattern cannot emerge from an interaction of a monotonic descending signal with feedback within the peripheral skeleto-motor system, then any simple form of the VITE model would be untenable.

Feldman (1986) presented a qualitative analysis suggesting that the peripheral system could compute the monotonic-to-multiphasic transform given appropriate parameters. The FLETE simulations indicate that a triphasic burst pattern of the correct form (large AG1 burst, then large ANT burst, then much smaller AG2 burst) does emerge when there is strong velocity-dependent feedback via the Ia pathway to alpha motoneurons and IaINs. This issue is currently controversial (see Berkinblit, Feldman, & Fukson, 1986) because bursts may also be observed in the absence of Ia feedback signals.

The controversy may stem from the fact that after their genesis by reactive, feedback systems within the peripheral FLETE circuits, the burst pattern may be "copied" into and amplified by a supplementary feedforward command channel by adaptive predictive learning of movement gains that is mediated by the cerebellum (Grossberg & Kuperstein, 1986). Thus after learning, the burst pattern can occur even after Ia afferent feedback is eliminated. In addition, simulations of the Renshaw-IaIN pathway suggest that bursting can emerge under certain conditions ("Renshaw size-principle") without participation by Ia feedback from spindle organs. Preliminary studies suggest that this effect could account for sub-bursts that have been observed in experiments utilizing EMG

recording techniques with high temporal resolution (Brown & Cooke, 1986), as well as bursts appearing in isometric studies (Gordon & Ghez, 1987). Even isometric studies present interpretive difficulties however, because intrafusal muscle activation via gamma motoneurons can evoke spindle discharge and Ia feedback in the absence of joint rotations. Detailed treatments of these simulations as well as a fuller report on refinements of the Table 2 simulations will appear elsewhere (Bullock & Grossberg, 1989a,b).

16. Conclusions

In the VITE circuit, a single GO signal sent in parallel to a large number of primed muscle-control channels can initiate goal-oriented synchronous movement, and control its rate without disrupting its form. In the FLETE circuit, a single co-contraction signal sent in parallel to a large number of muscle channels can control joint rigidity without disrupting postural stability. Both circuits clarify an old mystery in the theory of volitional action: if every act is so complex, why do volitional acts, or acts of "will," seem to be so simple?

Once such invariance-preserving components evolve, they can be expected to be incorporated into many subsequent evolutionary specializations (Bullock, 1987; Grossberg & Kuperstein, 1986, 1989; Lieberman, 1984; Powers, 1973; Simon, 1969). Here and elsewhere, we have argued that the VITE architecture or close variants may have been replicated across many systems which control phasic goal-oriented movements, including both arm and speech movements, and the circuit of Figure 8, which is mathematized in the FLETE model, is known to exist throughout the higher vertebrates. Similarly, the cerebellum serves as an adaptive gain control stage in a wide range of motor systems (Grossberg & Kuperstein, 1986, 1989; Ito, 1984; Kawato, Furukawa, & Suzuki, 1987). Despite initial appearances of overwhelming complexity, perhaps we may reasonably hope that the discovery of a modest number of robust and broadly applicable circuits will allow us to explain a large portion of the basic motor competence of higher vertebrate species.

Acknowledgements: We thank Carol Yanakakis for her expert help in preparing the manuscript.

References

Anderson, M. E., & Horak, F. B. (1985). Influence of the globus pallidus on arm movements in monkeys. III. Timing of movement-related information. *Journal of Neurophysiology, 54,* 433-448.

Beggs, W. D. A., & Howarth, C. I. (1972). The movement of the hand towards a target. *Quarterly Journal of Experimental Psychology, 24,* 448-453.

Berkinblit, M. B., Feldman, A. G., & Fukson, O. I. (1986). Adaptability of innate motor patterns and motor control mechanisms. *Behavioral and Brain Sciences, 9,* 585-638.

Bizzi, E., Accornero, N., Chapple, W., & Hogan, N. (1984). Posture control and trajectory formation during arm movement. *Journal of Neuroscience, 4 (11),* 2738-2744.

Bullock, D. (1987). Socializing the theory of intellectual development. In M. Chapman & R. A. Dixon (Eds.), *Meaning and the growth of understanding: Wittgenstein's significance for developmental psychology.* New York: Springer-Verlag, 187-218.

Bullock, D., Carpenter, G. A., & Grossberg, S. (1989). Self-organizing neural network architectures for adaptive pattern recognition and robotics. In V. Milutinovic & P. Antognetti (Eds.) *Neural networks: Concepts, applications and implementations.* Englewood Cliffs, NJ: Prentice Hall.

Bullock, D., & Grossberg, S. (1986). *Neural dynamics of planned arm movements: Synergies, invariants, and trajectory formation.* Paper presented at the symposium on Neural Models of Sensory-Motor Control at the annual meeting of the Society for Mathematical Psychology, Cambridge, MA, August 20.

Bullock, D., & Grossberg, S. (1988a). Neural dynamics of planned arm movements: Emergent invariants and speed-accuracy properties during trajectory formation. *Psychological Review, 95*(1), 49-90.

Bullock, D., & Grossberg, S. (1988b). The VITE model: A neural command circuit for generating arm and articulator trajectories. In J. A. S. Kelso, A. J. Mandel, & M. F. Shlesinger (Eds.), *Dynamic patterns in complex systems* (pp. 305-326). Singapore: World Scientific.

Bullock, D., & Grossberg, S. (1988c). Self-organizing neural architectures for eye movements, arm movements, and eye-arm coordination. In H. Haken (Ed.), *Neural and synergetic computers* (pp. 197-228). Berlin: Springer-Verlag.

Bullock, D., & Grossberg, S. (1988d). Neuromuscular realization of planned trajectories. *Neural Networks, 1,* Supplement 1, 329.

Bullock, D., & Grossberg, S. (1989a). *An opponent neuromuscular design for factorization of length and tension, I: Cocontraction, the size principle, and recurrent inhibition.* Manuscript submitted for publication.

Bullock, D., & Grossberg, S. (1989b). *An opponent neuromuscular design for factorization of length and tension, II: Force-time pattern generation during movement.* Manuscript submitted for publication.

Brown, S. H., & Cooke, J. D. (1986). Initial agonist burst is modified by perturbations preceding movement. *Brain Research, 377,* 311-322.

Carpenter, G. A., & Grossberg, S. (1987). Art 2: self-organization of stable category recognition codes for analog input patterns. *Applied Optics, 26*(23), 4919-4930.

Carpenter, G. A., & Grossberg, S. (1988). The ART of adaptive pattern recognition by a self-organizing neural network. *Computer, 21,* 77-88.

Cooke, J. D. (1980). The organization of simple, skilled movements. In G. E. Stelmach & J. Requin (Eds.), *Tutorials in motor behavior.* Amsterdam: North-Holland, 199-212.

Cooke, J. D., & Diggles, V. A. (1984). Rapid error correction during human arm movements: Evidence for central monitoring. *Journal of Motor Behavior, 16,* 348-363.

Cullheim, S., & Kellerth, J. O. (1978). A morphological study of the axons and recurrent axon collaterals of cat α-motoneurones supplying different functional types of muscle unit. *Journal of Physiology* (London), *281,* 301-313.

Eccles, J. C., Fatt, P., & Koketsu, K. (1954). Cholinergic and inhibitory synapses in a pathway from motor-axon collaterals to motoneurones. *Journal of Physiology* (London), *126,* 524-562.

Evarts, E. V., & Fromm, C. (1978). The pyramidal tract neuron as summing point in a closed-loop control system in the monkey. In J. E. Desmedt (Ed.), *Cerebral motor control in man: Long-loop mechanisms* (pp. 56-69). Basel, Switzerland: Karger.

Feldman, A. G. (1986). Once more on the equilibrium point hypothesis (λ model) for motor control. *Journal of Motor Behavior, 18,* 17-54.

Fisk, J. D., & Goodale, M. A. (1988). The effects of unilateral brain damage on visually guided reaching: hemispheric differences in the nature of the deficit. *Experimental Brain Research, 72,* 425-435.

Fitts, P. M. (1954). The information capacity of the human motor system in controlling the amplitude of movement. *Journal of Experimental Psychology, 47*(6), 381-391.

Freund, H. -J., & Büdingen, H. J. (1978). The relationship between speed and amplitude of the fastest voluntary contractions of human arm muscles. *Experimental Brain Research, 31,* 1-12.

Fromm, C., Haase, J., & Wolf, E. (1977). Depression of the recurrent inhibition of extensor motoneurones by the action of group II afferents. *Brain Research, 120,* 459-468.

Gahery, Y., & Massion, J. (1985). Co-ordination between posture and movement. In E. V. Evarts, S. P. Wise, & D. Bousfield (Eds.), *The motor system in neurobiology* (pp.121-125). Amsterdam: Elsevier.

Georgopoulos, A. P., Kalaska, J. F., & Massey, J. T. (1981). Spatial trajectories and reaction times of aimed movements: Effects of practice, uncertainty, and change in target location. *Journal of Neurophysiology, 46*(4), 725-743.

Georgopoulos, A. P., Kalaska, J. F., Caminiti, R., & Massey, J. T. (1984). The representation of movement direction in the motor cortex: Single cell and population studies. In G. M. Edelman, W. E. Gall, & W. M. Cowan (Eds.), *Dynamic aspects of neocortical function* (pp. 501-524). New York: Wiley.

Gielen, C. C. A. M., & Houk, J. C. (1987). A model of the motor servo: Incorporating nonlinear spindle receptor and muscle mechanical properties. *Biological Cybernetics, 57*, 217-231.

Goodale, M.A., Pelisson, D., & Prablanc, C. (1986). Large adjustments in visually guided reaching do not depend on vision of the hand or perception of target displacement. *Nature, 320*, 748-750.

Gordon, J., & Ghez, C. (1987). Trajectory control in targeted force impulses, III: Compensatory adjustments for initial errors. *Experimental Brain Research, 67*, 253-269.

Grossberg, S. (1970). Neural pattern discrimination. *Journal of Theoretical Biology, 27*, 291-337.

Grossberg, S. (1973). Contour enhancement, short-term memory, and constancies in reverberating neural networks. *Studies in Applied Mathematics, 52*, 217-257.

Grossberg, S. (1978). A theory of human memory: Self-organization and performance of sensory-motor codes, maps, and plans. In R. Rosen & F. Snell (Eds.), *Progress in theoretical biology, Vol. 5* (pp. 233-374). New York: Academic Press.

Grossberg, S. (1982). *Studies of mind and brain: Neural principles of learning, perception, development, cognition, and motor control.* Boston: Reidel Press.

Grossberg, S., & Kuperstein, M. (1986). *Neural dynamics of adaptive sensory-motor control: Ballistic eye movements.* Amsterdam: Elsevier/North-Holland.

Grossberg, S., & Kuperstein, M. (1989). *Neural dynamics of adaptive sensory-motor control: Expanded Edition.* New York: Pergamon Press.

Hasan, Z., & Enoka, R. M. (1985). Isometric torque-angle relationship and movement-related activity of human elbow flexors: implications for the equilibrium-point hypothesis. *Experimental Brain Research, 59*, 441-450.

Henatsch, H. D., Meyer-Lohmann, J., Windhorst, U., & Schmidt, J. (1986). Differential effects of stimulation of the cat's red nucleus on lumbar alpha motoneurons and their Renshaw cells. *Experimental Brain Research, 62*, 161-174.

Henneman, E. (1957). Relation between size of neurons and their susceptibility to discharge. *Science, 26*, 1345-1347.

Henneman, E. (1985). The size-principle: A deterministic output emerges from a set of probabilistic connections. *Journal of Experimental Biology, 115*, 105-112.

Hollerbach, J. M., Moore, S. P., & Atkeson, C. G. (1986). Workspace effect in arm movement kinematics derived by joint interpolation. In G. Gantchev, B. Dimitrov, & P. Gatev (Eds.), *Motor control*. Plenum Press.

Horak, F. B., & Anderson, M. E. (1984a). Influence of globus pallidus on arm movements in monkeys, I. Effects of kainic acid-induced lesions. *Journal of Neurophysiology, 52*, 290-304.

Horak, F. B., & Anderson, M. E. (1984b). Influence of globus pallidus on arm movements in monkeys, II. Effects of stimulation. *Journal of Neurophysiology, 52*, 305-322.

Houk, J. C., & Rymer, W. Z. (1981). Neural control of muscle length and tension. In *Handbook of physiology: The nervous system II* (pp. 257-322). Bethesda, MD: American Physiological Society.

Hultborn, H., Jankowska, E., & Lindström, S. (1971). Relative contribution from different nerves to recurrent depression of Ia IPSPs in motoneurones. *Journal of Physiology* (London), *215*, 637-664.

Hultborn, H., Lindström, S., & Wigström, H. (1979). On the function of recurrent inhibition in the spinal cord. *Experimental Brain Research, 37*, 399-403.

Humphrey, D. R., & Reed, D. J. (1983). Separate cortical systems for control of joint movement and joint stiffness: Reciprocal activation and coactivation of antagonist muscles. In J.E. Desmedt (Ed.), *Motor control mechanisms in health and disease* (pp. 347-372). New York: Raven Press.

Ito, M. (1984). *The cerebellum and neural control*. New York: Raven Press.

Kawato, M., Furukawa, K., & Suzuki, R. (1987). A hierarchical neural-network model for control and learning of voluntary movement. *Biological Cybernetics, 57*, 169-185.

Kuperstein, M. (1988). Neural network model for adaptive hand-eye coordination for single postures. *Science, 239*, 1308-1311.

Lestienne, F. (1979). Effects of inertial load and velocity on the braking process of voluntary limb movements. *Experimental Brain Research, 35*, 407-418.

Lieberman, P. (1984). *The biology and evolution of language*. Cambridge, MA: Harvard University Press.

Mateer, C. (1978). Asymmetric effects of thalamic stimulation on rate of speech. *Neuropsychologia, 16*, 497-499.

McMahon, T. A. (1984). *Muscles, reflexes, and locomotion*. Princeton, NJ: Princeton University Press.

Miller, S., & Scott, P. D. (1977). The spinal locomotor generator. *Experimental Brain Research, 30*, 387-403.

Mitchell, S. J., Richardson, R. T., Baker, F. H., & DeLong, M. R. (1987). The primate globus pallidus: neuronal activity related to direction of movement. *Experimental Brain Research, 68*, 491-505.

Moore, S. P., & Marteniuk, R. G. (1986). Kinematic and electromyographic changes that occur as a function of learning a time-constrained aiming task. *Journal of Motor Behavior, 18*, 397-426.

Neafsey, E. J., Hull, C. D., & Buchwald, N. A. (1978). Preparation for movement in the cat, II. Unit activity in the basal ganglia and thalamus. *Electroencephalography and Clinical Neurophysiology, 44*, 714-723.

Ostry, D. J., Cooke, J. D., & Munhall, K. G. (1987). Velocity curves of human arm and speech movements. *Experimental Brain Research, 68*, 37-46.

Passingham, R. E. (1987). From where does the motor cortex get its instructions? In S. P. Wise (Ed.), *Higher brain functions* (pp. 67-97). New York: Wiley.

Penney, J. B., & Young, A. B. (1983). Speculations on the functional anatomy of basal ganglia disorders. *Annual Review of Neuroscience, 6*, 73-94.

Piaget, J. (1963). *The origins of intelligence in children*. New York: Norton.

Pierrot-Deseilligny, E., & Morin, C. (1980). Evidence for supraspinal influences on Renshaw inhibition during motor activity in man. In J. E. Desmedt (Ed.), *Spinal and supraspinal mechanisms of voluntary motor control and locomotion*. Basel: Karger.

Pompeiano, O. (1984). Recurrent inhibition. In R.A. Davidoff (Ed.), *Handbook of the spinal cord, Vols. 2 and 3. Anatomy and physiology*. New York: Marcel Dekker.

Pompeiano, O., & Wand, P. (1976). The relative sensitivity of Renshaw cells to static and dynamic changes in muscle length. *Progress in Brain Research, 44*, 199-222.

Powers, W. T. (1973). *Behavior: The control of perception*. Chicago: Aldine.

Pratt, C. A., & Jordan, L. M. (1987). Ia inhibitory interneurons and Renshaw cells as contributors to the spinal mechanisms of fictive locomotion. *Journal of Neurophysiology, 57*, 56-71.

Rack, P. H. M., & Westbury, D. R. (1969). The effect of length and stimulus rate on the tension in the isometric cat soleus muscle. *Journal of Physiology, 204,* 443-460.

Renshaw, B. (1946). Central effects of centripetal impulses in axons of spinal ventral roots. *Journal of Neurophysiology, 9,* 191-204.

Renshaw, B. (1941). Influence of discharge of motoneurons upon excitation of neighboring motoneurons. *Journal of Neurophysiology, 4*, 167-183.

Ryall, R. W. (1970). Renshaw cell mediated inhibition of Renshaw cells: Patterns of excitation and inhibition from impulses in motor axon collaterals. *Journal of Neurophysiology, 33*, 257-270.

Schwartz, A. B., Kettner, R. E., & Georgopoulos, A. P. (1988). Primate motor cortex and free arm movements to visual targets in three-dimensional space. I. Relations between single cell discharge and direction of movement. *Journal of Neuroscience, 8*, 2913-2927.

Shepherd, G. M. (1979). *The synaptic organization of the brain.* New York: Oxford.

Sherrington, C. S. (1906). *The integrative action of the nervous system.* New Haven: Yale University Press.

Simon, H. A. (1969). *The sciences of the artificial.* Cambridge, MA: MIT Press.

Sparks, D. L., & Jay. M. F. (1986). The functional organization of the primate superior colliculus: A motor perspective. In H.-J. Freund, U. Butner, B. Cohen, & J. Noth (Eds.), *The oculomotor and skeletal-motor systems* (pp.235-241). Amsterdam: Elsevier.

Van Buren, J. M., Li, C. L., & Ojemann, G. A. (1966). The fronto-striatal arrest response in man. *Electroencephalography and Clinical Neurophysiology, 21*, 114-130.

Viallet, F., Trouche, E., Beaubaton, D., Nieoullon, A., & Legallet, E. (1983). Motor impairment after unilateral electrolytic lesions of the Substantia Nigra in baboons: Behavioral data with quantitative and kinematic analysis of a pointing movement. *Brain Research, 279*, 193-206.

Wand, P., & Pompeiano, O. (1979). Contribution of different size motoneurons to Renshaw cell discharge during stretch vibration reflexes. *Progress in Brain Research, 50*, 45-60.

Woodworth, R. S. (1899). The accuracy of voluntary movement. *Psychological Review, 3*, 1-114.

Wurtz, R. H., & Hikosaka, O. (1986). Role of the basal ganglia in the initiation of saccadic eye movements. In H.-J. Freund, U. Büttner, B. Cohen & J. Noth (Eds.), *Progress in brain research, Vol. 64* (pp. 175-190). Amsterdam: Elsevier.

Zelaznik, H. N., Schmidt, R. A., & Gielen, C. C. A. M. (1986). Kinematic properties of rapid aimed hand movements. *Journal of Motor Behavior, 18*, 353-372.